

A. R. Chakhmouradian · C. A. McCammon

Schorlomite: a discussion of the crystal chemistry, formula, and inter-species boundaries

Received: 30 September 2004 / Accepted: 2 March 2005 / Published online: 4 May 2005
© Springer-Verlag 2005

Abstract Examination of schorlomite from ijolite at Magnet Cove (USA) and silicocarbonatite at Afrikanda (Russia), using electron-microprobe and hydrogen analyses, X-ray diffraction and Mössbauer spectroscopy, shows the complexity of substitution mechanisms operating in Ti-rich garnets. These substitutions involve incorporation of Na in the eightfold-coordinated X site, Fe^{2+} and Mg in the octahedrally coordinated Y site, and Fe^{3+} , Al and Fe^{2+} in the tetrahedrally coordinated Z site. Substitutions $\text{Ti}^{4+}\text{Fe}^{3+}\text{Fe}^{3+}_{-1}\text{Si}_{-1}$ and $\text{Ti}^{4+}\text{Al}^{3+}\text{Fe}^{3+}_{-1}\text{Si}_{-1}$ are of major significance to the crystal chemistry of schorlomite, whereas Fe^{2+} enters the Z site in relatively minor quantities ($< 3\% \text{Fe}_{\Sigma}$). There is no evidence (either structural or indirect, such as discrepancies between the measured and calculated Fe^{2+} contents) for the presence of $^{6}\text{Ti}^{3+}$ or $^{4}\text{Ti}^{4+}$ in schorlomite. The simplified general formula of schorlomite can be written as $\text{Ca}_3\text{Ti}^{4+}_2[\text{Si}_{3-x}(\text{Fe}^{3+}, \text{Al}, \text{Fe}^{2+})_x\text{O}_{12}]$, keeping in mind that the notion of end-member composition is inapplicable to this mineral. In the published analyses of schorlomite with low to moderate Zr contents, x ranges from 0.6 to 1.0, i.e. Ti^{4+} in the Y site is < 2 and accompanied by appreciable amounts of lower-charged cations (in particular, Fe^{3+} , Fe^{2+} and Mg). For classification purposes, the mole percentage of schorlomite can be determined as the amount of $^{6}\text{Ti}^{4+}$, balanced by substitutions in the Z site, relative to the total occupancy in the Y site: $(^{6}\text{Ti}^{4+}_{-1} + ^{6}\text{Fe}^{2+}_{-1} + ^{6}\text{Mg}^{2+}_{-1} + ^{8}\text{Na}^+) / 2$. In addition to the predominant schorlomite component, the crystals

examined in this work contain significant ($> 15 \text{ mol.}\%$) proportions of andradite ($\text{Ca}_3\text{Fe}^{3+}_2\text{Si}_3\text{O}_{12}$), morimotoite ($\text{Ca}_3\text{Fe}^{2+}\text{TiSi}_3\text{O}_{12}$), and $\text{Ca}_3\text{MgTiSi}_3\text{O}_{12}$. The importance of accurate quantitative determination and assignment of Fe, Ti and other cations to the crystallographic sites for petrogenetic studies is discussed.

Keywords Schorlomite · Garnet · Mössbauer spectroscopy · Crystal-structure refinement

Introduction

Very few minerals have generated as much nomenclatural controversy as schorlomite. This Ti-rich member of the garnet family ($^{8}\text{X}_3^{6}\text{Y}_2^{4}\text{Z}_3\text{O}_{12}$) was discovered in ijolite (?) at the Magnet Cove alkaline complex, Hot Spring County, Arkansas (Shepard 1846). In 1852, a similar mineral was reported by Nordenskiöld from foidolitic rocks of the Iivaara complex (Finland) under the name iivaarite (Lehijarvi 1960, p. 51). The latter name was subsequently discarded in favor of schorlomite which had the historical priority. In the past 50 years, Ti-rich garnets have been observed in a large variety of rocks, including alkali-feldspar and nepheline syenites, phonolites, foidolites (especially melteigites and ijolites), nephelinites, melilitolites (*sensu lato*), melilitites, plutonic ultramafic rocks of alkaline affinity, carbonatites, phoscorites, alnöites, kimberlites, orangeites, fenites, and diverse calc-silicate metamorphic parageneses (principally, rodingites and skarns). A comprehensive list of relevant literature references is available from the corresponding author upon request. The composition of titaniferous garnets and their paragenetic relationships are considered important petrogenetic indicators. They have been used, for example, for constraining $a(\text{SiO}_2)$ and $f(\text{O}_2)$ in magmas and hydrothermal fluids (Russell et al. 1999), mobility of Ti during metamorphism (Müntener and Hermann 1994), provenance of metasomatic fluids (Ulrych et al. 1994), and magma differenti-

A. R. Chakhmouradian (✉)
Department of Geological Sciences,
University of Manitoba, Winnipeg,
MB, R3T 2N2, Canada
E-mail: chakhmou@ms.umanitoba.ca
Tel.: +1-204-4747278
Fax: +1-204-4747623

C. A. McCammon
Bayerisches Geoinstitut,
Universität Bayreuth,
95440 Bayreuth, Germany

ation processes (Brod et al. 2003). Unfortunately, many of these studies exclusively use electron-microprobe data to derive element concentrations or element ratios of petrogenetic significance. The shortcomings of this simplistic approach are discussed below.

Depending largely on their Ti content, titaniferous garnets have been referred to as schorlomite or titanian andradite (a.k.a. “melanite”). There is a continuous series of compositions from Ti-free andradite ($\text{Ca}_3\text{Fe}^{3+}_2\text{Si}_3\text{O}_{12}$) to calcic garnets with > 20 wt% TiO_2 (e.g., Grapes et al. 1979), but examples containing > 18 wt% TiO_2 are exceptionally rare. A garnet with ca. 18.5 wt% TiO_2 and apparent enrichment in $\text{Ca}_3(\text{Ti}^{4+}\text{Fe}^{2+})\text{Si}_3\text{O}_{12}$ component was described recently as the new mineral morimotoite (Henmi et al. 1995). However, neither crystal-structure refinement, nor spectroscopic investigation of this material have been attempted to confirm the proposed assignment of cations to crystallographic sites, or the proportion between Fe and Ti in different oxidation states (for more detailed discussions, see Fehr and Amthauer 1996; Rass 1997; Armbruster et al. 1998, p. 920). Clearly, a re-examination of the type-material morimotoite is warranted to validate it as a mineral species distinct from schorlomite.

To date, there has been no consensus as to where the boundaries between schorlomite and other garnet species should be drawn, or what to consider the end-member formula of the latter. For instance, the X-ray powder diffraction (XRD) data reported for schorlomite in PDF 33-0285 were obtained on material from San Benito, California. However, garnets from this locality are invariably referred to in the literature as titanian andradite (e.g., Moore and White 1971; Armbruster et al. 1998). Further, there are cases where schorlomite has been single-handedly discarded as a valid mineral species (e.g., Roberts et al. 1974), or garnets with identical Ti contents referred to as both schorlomite and melanite (e.g., Schwartz et al. 1980). Some examples of the previously proposed definitions of schorlomite are compiled in Table 1.

To a great extent, the controversy surrounding schorlomite is due to the complex nature of atomic substitutions responsible for the incorporation of Ti in the garnet structure (see below). The available compositional data (principally, inter-element correlations) indicate that these substitutions typically involve more than one cation site (e.g., Scordari et al. 1999). The principal sources of uncertainty are:

1. Lack of any structural information for the majority of Ti-rich garnets described in the literature, resulting in ambiguous assignment of elements to specific cation sites. In particular, many contemporary works rely on the definitions proposed in the older studies, which involved neither accurate structural refinement nor in-depth spectroscopic analysis of schorlomite (Table 1).
2. Different individual approaches to recalculation of garnet compositions to end-member proportions

Table 1 Definition of schorlomite: some examples from the literature

Proposed definition, formula ^a , or compositional criterion	Reference
> 15 wt% TiO_2	Zedlitz (1933)
> 0.75 apfu Ti^b (> ca. 11.5 wt% TiO_2)	Kukhareno and Bagdasarov (1962)
$\text{Ca}_3\text{Ti}^{4+}_2(\text{Fe}^{3+}_2\text{Si})\text{O}_{12}$	Ito and Frondel (1967)
$\text{Ca}_3\text{Ti}_2(\text{Fe}^{3+}_2\text{Ti})\text{O}_{12}$	Rickwood (1968)
> 0.5 apfu Ti (> ca. 8 wt% TiO)	Howie and Woolley (1968)
$\text{Ca}_3(\text{Al,Fe,Ti})_2(\text{Si,Ti})_3\text{O}_{12}$	Yakovlevskaya (1972)
Ti-rich andradite	Roberts et al. (1974)
$^{16}\text{Ti} > ^{16}\text{Fe}^{3+}$	Deer et al. (1982)
$\text{Ca}_3(\text{Fe,Ti})_2(\text{Si,Ti})_3\text{O}_{12}$	PDF 33-0285
$\text{Ca}_3(\text{Ti}^{4+}, \text{Fe}^{3+})_2(\text{Si, Fe}^{3+})_3\text{O}_{12}$	Anthony et al. (1995)
$\text{Ca}_3(\text{Ti}^{4+}, \text{Fe}^{3+}, \text{Al})_2(\text{Si, Fe}^{3+}, \text{Fe}^{2+})_3\text{O}_{12}$	Gaines et al. (1997)
$\text{Ca}_3\text{Ti}^{3+}_2\text{Ti}^{4+}_3\text{O}_{12}$	Rass and Dubrovinskii (1997)
$\text{Ca}_3(\text{Ti, Fe}^{2+})_2[(\text{SiO}_4)_2(\text{OH})_4]$	Yakovenchuk et al. (1999)
$\text{Ca}_3\text{Ti}_2(\text{Al}_2\text{Si})\text{O}_{12}$	Gwalani et al. (2000)

Definitions most commonly used in the mineralogical literature are given in bold

^aFor clarity, cations accommodated in the same site are enclosed in parentheses

^bAtoms per formula unit (apfu) relative to 12 atoms of oxygen

(arising from the multiplicity of substitution mechanisms and, hence, potential end-members).

3. Possible presence of Ti^{3+} in garnets (e.g., Schwartz et al. 1980), resulting in incorrect estimations of $\text{Fe}^{2+}/\text{Fe}^{3+}$ ratio from electron-microprobe data (i.e. higher-than-actual Fe^{2+} contents).
4. Presence of $(\text{OH})^{1-}$ in some titaniferous garnets (e.g., Lager et al. 1989; Müntener and Hermann 1994), resulting in incorrect estimations of $\text{Fe}^{2+}/\text{Fe}^{3+}$ ratio from electron-microprobe data (i.e. lower-than-actual Fe^{2+} contents).
5. Significant intragranular variation in Ti, Fe and Si contents commonly exhibited by Ti-rich garnets (e.g., Flohr and Ross 1989; Dawson et al. 1995; Gwalani et al. 2000).

The major objective of the present work is to provide an integrated analysis of the crystal chemistry of schorlomite, including material from the type locality at Magnet Cove. A similar assessment has been recently done for titanian andradite (Armbruster et al. 1998), but not for compositions with > 13 wt% TiO_2 . We shall also address discrepancies in the previously published interpretations of Ti incorporation in garnets, and attempt to redefine schorlomite in the context of these new and existing data. For this purpose, we examined a collection of eight garnets (four from Magnet Cove, and four from northwestern Russia), and selected for more detailed investigation two crystals that differ in provenance, have relatively homogeneous composition, lack minute inclusions of other minerals, and would be classified as schorlomite, regardless of which of the existing classification schemes was chosen (Table 1).

Crystal chemistry of Ti-rich garnets: background information

At ambient pressures, only Fe-dominant granditic garnets contain appreciable levels of Ti. The crystal-chemical reasons for such selectivity were addressed in detail by Armbruster et al. (1998). Ti in the structure of natural garnets (Fig. 1) is typically interpreted as tetravalent and accommodated predominantly in the octahedrally coordinated Y site (ibid.; Amthauer et al. 1977; Locock et al. 1995). In a number of studies, the presence of significant $^{[6]}\text{Ti}^{3+}$ (up to 50% of total Ti) has been advocated on the basis of discrepancies between the $\text{Fe}^{2+}/\text{Fe}^{3+}$ values obtained by chemical and Mössbauer methods (Schwartz et al. 1980; Wu and Mu 1986), or X-ray photoelectron spectra (Malitesta et al. 1995). In these studies, Ti^{4+} is assigned to both Y and tetrahedrally coordinated Z sites. In contrast, the near-edge X-ray absorption spectra revealed no compelling evidence for detectable $^{[6]}\text{Ti}^{3+}$ or $^{[4]}\text{Ti}^{4+}$ in garnets with a wide range of Ti contents (Waychunas 1987; Locock et al. 1995). This is in agreement with the experimental data of Povarennykh and Shabalin (1983) showing that $^{[4]}\text{Ti}^{4+}$ occurs only in garnets with insufficient Fe^{3+} to completely fill the Z sites. Synthetic $\text{Ca}_3\text{Ti}^{4+}_2(\text{Fe}^{3+}_2\text{Si})\text{O}_{12}$, equivalent to one of the proposed end-member compositions for schorlomite, appears to contain only $^{[6]}\text{Ti}^{4+}$ (ibid.). Waychunas (1987, p. 89) also suggested that “ Ti^{4+} can enter tetrahedral coordination in special cases where Si^{4+} , Al^{3+} , or Fe^{3+} are unavailable in

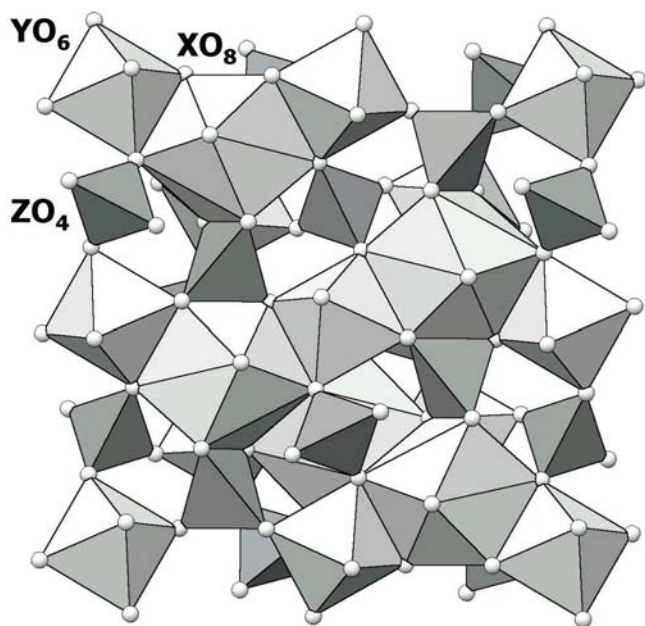


Fig. 1 Crystal structure of garnet as seen down the [100] axis (slice ca. $16 \times 16 \times 8$ Å is shown). Note large XO_8 polyhedra sharing edges with YO_6 octahedra and ZO_4 tetrahedra (shaded), and zigzag chains of corner-sharing YO_6 and ZO_4 parallel to [100]. See Discussion for the potential routes of electron transfer among $^{[8]}\text{Fe}^{2+}$, $^{[6]}\text{Fe}^{2+}$ and $^{[4]}\text{Fe}^{3+}$

sufficient amounts.” Clearly, very few natural environments would meet these “special” requirements. Moore and White (1971) ruled out $^{[4]}\text{Ti}^{4+}$, but proposed the existence of both $^{[6]}\text{Ti}^{3+}$ and $^{[6]}\text{Ti}^{4+}$ in schorlomite from Magnet Cove and Iivaara. According to Armbruster et al. (1998), the presence of $^{[6]}\text{Ti}^{3+}$ in a garnet would be evident from a lower-than-expected (i.e., for the given Ti content) unit-cell parameter, and X-Y interatomic distance.

Incorporation of Ti^{4+} in the garnet structure must be accompanied by substitution of the proportional amount of $^{[8]}\text{Ca}$, $^{[6]}\text{Fe}^{3+}$ or $^{[4]}\text{Si}$ by lower-valence cations. Of all alkalis, only Na is present in Ti-rich garnets in amounts detectable by EMPA. Although this element is rarely included in garnet analyses, the available data seem to indicate that the Na_2O content typically does not exceed 0.4 wt%, even in the most Ti-rich compositions (Flohr and Ross 1989; Dawson et al. 1995; Locock et al. 1995; Gwalani et al. 2000). The highest Na_2O content reported to date is ca. 0.7 wt% in samples from Ozeraya Varaka in Russia (Yakovlevskaya 1972) and Swartruggens in South Africa (described as a Ca–Ti–Fe silicate: Hammond and Mitchell 2002). However, even in the latter cases, the $\text{NaTi}^{4+}\text{Ca}_{-1}\text{Fe}^{3+}_{-1}$ substitution accounts for only about 0.13 apfu Ti.

Substitutions in the Y site are more extensive, but effectively limited to $\text{Fe}^{2+}\text{Ti}^{4+}\text{Fe}^{3+}_{-2}$ (delineating a trend toward the putative morimotoite end-member) and $\text{MgTi}^{4+}\text{Fe}^{3+}_{-2}$. The range of FeO contents reported in the literature for Ti-rich garnets is from nil to 9.8 wt% in morimotoite (Henmi et al. 1995). In this and most other studies, the FeO value was simply calculated from the total Fe content on the basis of ideal stoichiometry and assuming that neither Ti^{3+} nor $(\text{OH})^{1-}$ were present in the sample (see Introduction). Where structural information is available, Fe^{2+} may be assigned to X and Y (Schwartz et al. 1980; Scordari et al. 1999), Y and Z (Locock et al. 1995), or all three cation sites (Kühberger et al. 1989). Hence, it is difficult to assess the actual extent of morimotoite substitution in natural garnets. The $\text{MgTi}^{4+}\text{Fe}^{3+}_{-2}$ substitution is comparatively less important because the MgO content rarely exceeds 1.4 wt% (references as above). One notable exception is zirconian schorlomite from Polino (Italy) containing 2.0–2.6 wt% MgO (Lupini et al. 1992). Considering that in all these cases, the X site is almost completely occupied by Ca (\pm minor Na, Mn, Fe^{2+} and REE), at least 0.30 apfu Ti can potentially be accommodated in the garnet structure via the $\text{MgTi}^{4+}\text{Fe}^{3+}_{-2}$ substitution.

Cation substitutions in the Z site are the most controversial aspect of the crystal chemistry of Ti-rich garnets. The overwhelming majority of studies agree that $^{[4]}\text{Fe}^{3+}$ is one of the major substituents for Si (e.g., Amthauer et al. 1977; Schwartz et al. 1980; Wu and Mu 1986), but it is still debated what other cations can be accommodated at this site in significant amounts. Huggins et al. (1977), Schwartz et al. (1980) and several other workers proposed that Al^{3+} and Ti^{4+} also substitute for

Si, but disagreed on the relative preference of these cations for the Z site. The three contrasting models are $\text{Al}^{3+} \geq \text{Fe}^{3+} > \text{Ti}^{4+}$ (Huggins et al. 1977), $\text{Fe}^{3+} > (\text{Al}^{3+}, \text{Ti}^{4+})$ (Schwartz et al. 1980; Wu and Mu 1986), and $\text{Fe}^{3+} \geq \text{Ti}^{4+} > \text{Al}^{3+}$ (Scordari et al. 1999). The significance of Al-for-Si substitution is believed to increase with enrichment of the garnet in Zr owing to structural constraints (e.g., Armbruster et al. 1998). In a number of studies, $^{54}\text{Fe}^{2+}$ has been identified as a species next in abundance to $^{54}\text{Fe}^{3+}$ (Amthauer et al. 1977; Kühberger et al. 1989; Locock et al. 1995). Because ^{57}Fe Mössbauer spectroscopy was utilized in most of the aforementioned studies, the observed discrepancy in results can only be explained by ambiguities in interpretation of the spectroscopic data (see Discussion).

In addition to the work cited above, there have been many publications where the mechanism of Ti incorporation in the garnet structure is analyzed exclusively on the basis of inter-element correlations (e.g., Russell et al. 1999; Gwalani et al. 2000). We do not discuss these data here because cation substitutions in Ti-rich garnets affect two crystallographic sites simultaneously, and involve elements that can potentially enter more than one site (e.g., Fe, Ti, Al, Mg). One typical example is a negative correlation between Ti and Si commonly interpreted to indicate a simple homovalent substitution between these two elements (ibid.). Note, however, that substitution $\text{Ti}^{4+}\text{Fe}^{3+}\text{Fe}^{3+}_{-1}\text{Si}^{4+}_{-1}$ will also generate an antipathetic Ti/Si trend, regardless of the fact that no Ti is accommodated in the Z site. Clearly, crystallographic and spectroscopic data are required in addition to chemical analyses to constrain the distribution of Ti, Fe and other elements among the different cation sites.

Sample description and analytical methods

Sample AF-05 is a large (~2 cm across) black dodecahedral crystal collected from silicocarbonatite at Afrikanda, Kola Peninsula. Associated minerals are magnesiohastingsite, calcite, magnetite, perovskite, titanite, clinocllore and various Zr phases. Further details on this paragenesis and the geology of Afrikanda are

provided elsewhere (Chakhmouradian and Zaitsev 2002, 2004). In thin section, this garnet is reddish brown and isotropic, with very subtle oscillatory-type zoning involving minor variations in Ti (Table 2); this zoning is undetectable in back-scattered-electron images (BSE). The primary Ti-rich garnet is overgrown by thin mantles of titanian andradite with < 8 wt% TiO_2 (ibid.). These late-stage overgrowths are optically distinct from the primary garnet and were discarded during the sample preparation.

Sample MC-04, donated by Howard (Arkansas Geological Commission), is a crystal fragment collected from regolith covering garnet-bearing ijolites in the western part of the Magnet Cove complex. A detailed description of the ijolites and Magnet Cove complex as a whole is given in Flohr and Ross (1989). Garnet MC-04 is macroscopically black, and dark reddish brown and isotropic in thin section. Zoning is undetectable either optically or in BSE.

Both samples were sawn approximately in half; one of the off-cuts was used for the preparation of polished sections, and the other crushed and sieved to fragments ranging between 0.03 mm and 0.80 mm in size. From these, homogeneous fragments were hand-picked for crystal-structure, spectroscopic and X-ray powder diffraction (XRD) studies, and for hydrogen analysis. The polished sections were used for electron-microprobe analysis (EMPA). The composition of both garnets (Table 2) was determined by wavelength-dispersive X-ray spectrometry using a Cameca SX-50 instrument operated at 15 kV and 20 nA, with a beam diameter of 5 μm . The following natural and synthetic standards were employed for the analysis: albite (Na), andalusite (Al), diopside (Ca, Si), fayalite (Fe), forsterite (Mg), spessartine (Mn), titanite (Ti), zircon (Zr), and MnNb_2O_6 (Nb). The $K\alpha$ line was used for all elements, except Zr and Nb ($L\alpha$ line for both). V was not detected in either of the samples. The hydrogen content was determined in pulverized samples by combustion in an O_2 stream using a CEC 240-XA elemental analyzer. Mg perchlorate was used for hydrogen removal.

Small fragments of MC-04 and AF-05 chosen for the structural analysis were ground to spheres 150–180 μm

Table 2 Representative electron-microprobe analyses of schorlomite from Afrikanda and Magnet Cove

Wt%	Sample AF-05			Sample MC-04		
	Low-Ti	High-Ti	Average (<i>n</i> = 10)	Low-Ti	High-Ti	Average (<i>n</i> = 7)
Na_2O	0.08	0.32	0.14	0.09	0.09	0.12
CaO	31.71	31.79	31.86	31.63	31.54	31.53
MnO	0.27	0.31	0.28	0.44	0.48	0.47
MgO	1.28	1.10	1.23	1.22	1.21	1.23
Al_2O_3	2.48	1.49	2.20	1.53	1.60	1.55
$(\text{Fe}_2\text{O}_3)_\Sigma$	20.43	20.47	20.48	20.59	20.89	20.65
SiO_2	27.39	26.89	27.11	26.29	26.16	26.22
TiO_2	13.52	15.52	15.02	15.74	16.52	16.24
ZrO_2	2.88	2.31	1.93	1.39	1.31	1.34
Nb_2O_5	0.15	0.07	0.07	0.12	ND	0.05
Total	100.19	100.27	100.32	99.04	99.80	99.40

across, and mounted on a Bruker P4 automated four-circle diffractometer equipped with a serial detector and MoK α X-ray source. Ten reflections over the range $15^\circ \leq 2\theta \leq 60^\circ$ were automatically centered, and the unit-cell parameters and orientation matrices were determined by least-squares refinement of the setting angles. A total of 1,489 reflections was measured between 4° and $60^\circ 2\theta$, in the index range $0 \leq (h, k, l) \leq 17$, using a variable scan speed ($3\text{--}30^\circ 2\theta/\text{min}$). Data for empirical absorption correction were collected in ψ -scan mode at intervals of 10° along the diffraction vector, and the crystal shape was modeled as an ellipse. The same method was then used to correct the θ - 2θ data. The data were corrected for Lorentz, polarization and background effects, and reduced to structure factors. All 224 unique reflections were classed as observed. The structure was refined in space group Ia3d using the Bruker SHELXL-93 software. Scattering factors were taken from Ibers and Hamilton (1992). Further information relevant to the single-crystal X-ray data collection and structure refinements is provided in Table 3.

Two samples selected for Mössbauer studies were gently ground to powder in an agate mortar with acetone mixed with benzophenone, and loaded into a sample holder. The sample weight was determined based on the iron composition such that the dimensionless effective sample thickness was equal to 2 (corresponds to 5 mg Fe/cm^2). Mössbauer spectra were recorded in transmission mode on a constant acceleration Mössbauer spectrometer with a nominal $50 \text{ mCi } ^{57}\text{Co}$ source in a 6 micron Rh matrix. Spectra were recorded at room temperature (293 K) and 80 K, the latter using a continuous-flow cryostat with the sample in nitrogen vapor. The velocity scale was calibrated relative to $25 \mu\text{m } \alpha\text{-Fe}$ foil using the positions certified for National Bureau of Standards standard reference material no. 1541; line

widths of 0.28 mm/s for the outer lines of $\alpha\text{-Fe}$ were obtained at room temperature. The spectra were fitted using the commercially available fitting program NORMOS written by Brand (distributed by Wissenschaftliche Elektronik GmbH, Germany). The spectra took one day each to collect.

Small crystal fragments of AF-05 were ground in acetone in an agate mortar, the powder loaded in an aluminum sample holder and gently compressed with a glass slide. X-ray powder diffraction (XRD) data were obtained using a Phillips 3710 diffractometer (CuK α radiation) operated at 30 mA and 40 kV in a step-scanning mode. The data were collected over a 2θ range of $20^\circ\text{--}140^\circ$ with a step size of $0.02^\circ 2\theta$ and a step time of 2 s. The unit-cell parameter was refined using the UnitCell software (Holland and Redfern 1997), which utilizes a non-linear least-squares method.

Results

Chemical composition

EMPA confirmed that the Magnet Cove sample is essentially homogeneous in composition (Table 2). It contains lower Al and higher Zr contents in comparison with the ijolitic schorlomite studied by Flohr and Ross (1989). None of the three CHN analyses performed on this material detected hydrogen. Sample AF-05 is slightly poorer in Ti, and richer in Si, Al and Zr relative to MC-04. The Afrikanda garnet also shows a wider compositional range (Table 2), but the bulk of the crystal contains 14.9–15.4 wt% TiO₂. Sample AF-05 contains an amount of hydrogen equivalent to 0.21 wt% H₂O (average of three measurements). The average analyses of both garnets have $>15 \text{ wt\% TiO}_2$ (Table 2) and, thus, correspond to schorlomite according to the classification criteria of Zedlitz (1933), Kukharenko and Bagdasarov (1962), and Howie and Woolley (1968) (Table 1). Both samples (especially MC-04) are similar in chemistry to schorlomite from the Ice River complex (Canada), studied by Locock et al. (1995).

Crystal structure

The topology of garnet structure (Fig. 1) is described elsewhere (e.g., Schwartz et al. 1980), and is not discussed here in any detail. The atomic positional and displacement parameters, as well as selected interatomic distances of the examined schorlomite samples are listed in Table 4. The oxygen positions do not deviate significantly from those reported in the literature for Ti-rich garnets from other localities (e.g., Armbruster et al. 1998, their Table 3). The calculated X-Y distance, and the length of the polyhedral edge shared between XO₈ and YO₆ (Table 4) correlate with the general trends observed by Armbruster et al. (1998). There is no indication of X-Y or unit-cell “contraction” that would

Table 3 Details of crystal-structure refinement for schorlomite from Afrikanda and Magnet Cove

Space group	Ia3d		Ia3d
Unit-cell parameters:			
AF-05	a 12.1464(5) Å	MC-04	a 12.1524(10) Å
	V 1792.0(2) Å ³		V 1794.7(4) Å ³
Calculated density (D_x)			
AF-05	3.787(1) g/cm ³	MC-04	3.800(1) g/cm ³
Linear absorption coefficient (μ)			
AF-05	5.03 mm ⁻¹	MC-04	5.02 mm ⁻¹
R1			
AF-05	0.0206	MC-04	0.0189
	for 208	for 207	
	$ F_o > 4\sigma F$	$ F_o > 4\sigma F$	
	0.0213	0.0191	
	for all 224	for all 224	
	unique data	unique data	
wR2			
AF-05	0.0309	MC-04	0.0302
Goodness-of-fit			
AF-05	1.240	MC-04	1.254
Difference peaks			
AF-05	-0.19,	MC-04	-0.19,
	+0.21 e ⁻ Å ⁻³		+0.24 e ⁻ Å ⁻³

suggest the presence of substantial $^{6}\text{Ti}^{3+}$. Good agreement between the measured and calculated $\text{Fe}^{2+}/\text{Fe}_{\Sigma}$ values (see Discussion) confirms the paucity (or absence) of Ti^{3+} in our samples.

To constrain the distribution of cations among the different sites, we used the refined electron density at each site (expressed in electrons per formula unit, or epfu), cation–oxygen distances (Table 4), and the Mössbauer data (see below). As could be expected, the electron density in both garnets is significantly lower in the Y site (≤ 46.7) and higher in the Z site (≥ 47.5) relative to the case of full occupancy of these sites by Fe^{3+} and Si, respectively. The X site contains more electrons than the ideal value (60), but the deviation is within 2% of the latter. In AF-05 and MC-04, the Z–O distance is larger, whereas Y–O is slightly shorter than the corresponding distances in andradite (ca. 1.65 and 2.02 Å; Armbruster and Geiger 1993). The X–O distance in both garnets deviates from the Ca–O distance in andradite by less than 0.5%. These data indicate that the samples studied contain a significant proportion of cation(s) lighter and somewhat smaller than Fe^{3+} in the Y site, as well as of heavier and larger cation(s) substituting for Si in the Z site; the X site is only subtly affected by substitution of Ca by heavier elements.

Mössbauer spectroscopy

The spectra at room temperature consist of two prominent doublets with an extremely broad absorption seen on the high-velocity shoulder (Fig. 2). In order to resolve the individual components more effectively, a spectrum of each sample was taken at 80 K. The two

Table 4 Structural parameters and key interatomic distances for schorlomite from Afrikanda and Magnet Cove

Site	Coordinates	U_{eq}	Interatomic distances (Å):	
Sample AF-05				
X	(1/8, 0, 1/4)	0.0110(2)	X–O ($\times 4$)	2.368(1)
Y	(0, 0, 0)	0.0074(2)	X–O' ($\times 4$)	2.515(1)
Z	(3/8, 0, 1/4)	0.0077(2)	X–O	2.442(1)
			Y–O ($\times 6$)	2.006(1)
O		0.0122(3)	Z–O ($\times 4$)	1.689(1)
x	0.0373(1)		X–Y	3.395
y	0.0483(1)		shared edge XO ₈ /YO ₆	2.843(1)
z	0.65348(9)		shared edge XO ₈ /ZO ₄	2.622(1)
Sample MC-04				
X	(1/8, 0, 1/4)	0.0097(2)	X–O ($\times 4$)	2.367(1)
Y	(0, 0, 0)	0.0059(2)	X–O' ($\times 4$)	2.517(1)
Z	(3/8, 0, 1/4)	0.0060(2)	X–O	2.442(1)
			Y–O ($\times 6$)	2.005(1)
O		0.0112(3)	Z–O ($\times 4$)	1.693(1)
x	0.03706(9)		X–Y	3.397
y	0.04822(9)		Shared edge XO ₈ /YO ₆	2.839(1)
z	0.65335(8)		shared edge XO ₈ /ZO ₄	2.625(1)

spectra collected at 80 K are similar, and can be resolved into four main doublets, which from center-shift values can be assigned to Fe^{3+} and Fe^{2+} (two doublets each) (Fig. 3). The residuals are large when purely Lorentzian line shapes are used to fit the spectra, whereas a combination of Lorentzian and Voigt lines gives significantly smaller residuals. Several models were explored to determine the sensitivity of parameters. The line positions are relatively insensitive to the fitting model, while the relative areas of the Fe^{3+} doublets are slightly more sensitive. The overall $\text{Fe}^{2+}/\text{Fe}^{3+}$ ratio is relatively model-independent. The final fitting model was chosen to be the one that was most simple, yet realistic, and fit the data: Lorentzian doublets for Fe^{2+} absorption and Voigt doublets for Fe^{3+} absorption with the linewidths of the Voigt components constrained to the natural linewidth (0.195 mm/s). The conventional constraints among components were applied to all doublets (equal component widths and areas). The uncertainties in the hyperfine parameters were estimated based on their variation among models.

Two models, each with four doublets, were explored for fitting the 80 K spectra. The positions of three of the

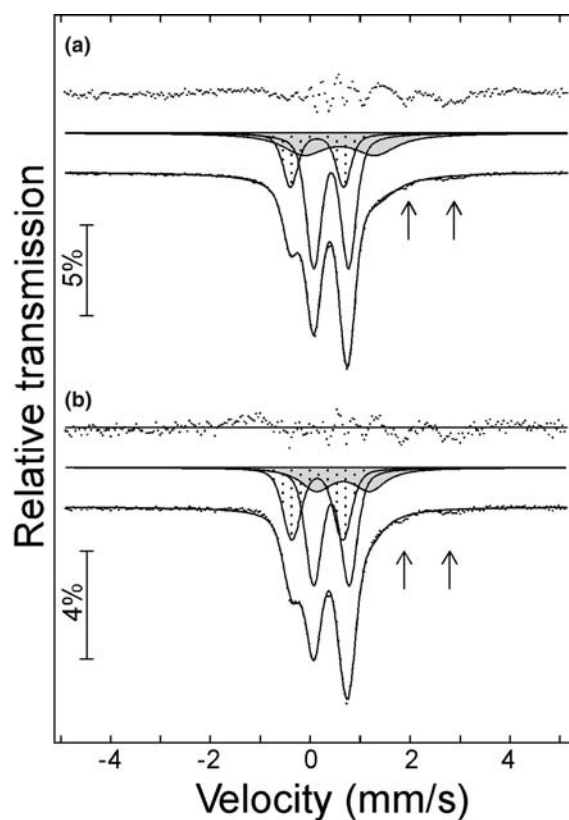


Fig. 2 Mössbauer spectra of schorlomite samples at room temperature: **a** AF-05, **b** MC-04. The spectra were fit to three doublets corresponding to $^{4}\text{Fe}^{3+}$ (speckled), $^{6}\text{Fe}^{3+}$ (unshaded) and thermally activated electron transfer (grey). Small peaks corresponding to $^{8}\text{Fe}^{2+}$ and $^{4}\text{Fe}^{2+}$ are indicated by arrows, but were not fit due to their weak intensity. The fit should be considered approximate because the exact line shape for electron transfer is unknown

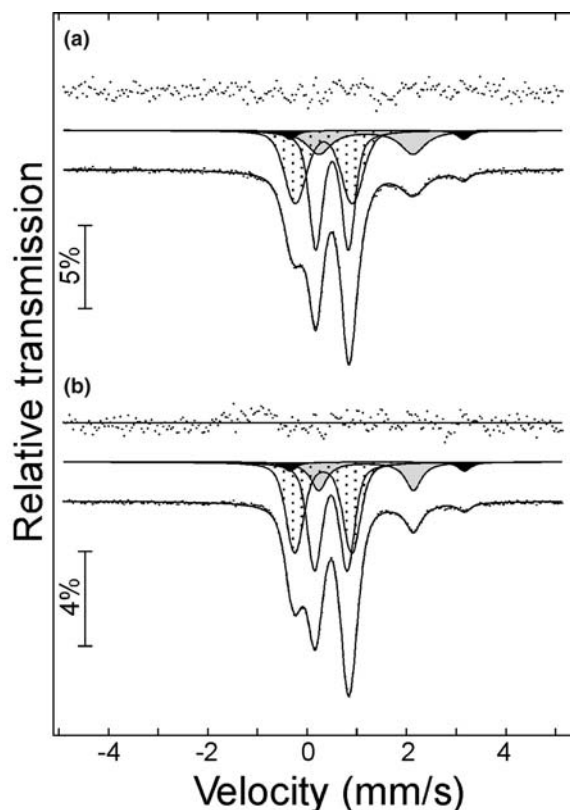


Fig. 3 Mössbauer spectra of schorlomite samples at 80 K: **a** AF-05, **b** MC-04. The spectra were fit to four doublets corresponding to $^{44}\text{Fe}^{3+}$ (speckled), $^{66}\text{Fe}^{3+}$ (unshaded), $^{66}\text{Fe}^{2+}$ (grey) and $^{88}\text{Fe}^{2+}$ (black). Hyperfine parameters are listed in Table 5 as model #2

doublets were essentially insensitive to the fitting model, while the position of the fourth doublet varied. The first model yields a lower center shift for the fourth doublet (ca. 1.09 mm/s relative to $\alpha\text{-Fe}$) relative to the second model (ca. 1.19 mm/s). Both models give equally good statistical fits to the data, and the positions and intensities of the other three doublets in the spectrum are essentially unchanged between the two models (Table 5). The room temperature spectra differ from the 80 K spectra in that the high-velocity component of the fourth doublet is absent, and is replaced by an extremely broad absorption on the high-velocity shoulder of the Fe^{3+} doublets. As a first approximation, we fit three doublets to the room-temperature spectra: two Voigt doublets corresponding to Fe^{3+} , and one broad Lorentzian doublet representing the remainder of spectral absorption (Fig. 3).

X-ray powder diffraction

The XRD data reported for schorlomite in PDF 33-285 were obtained on material from San Benito, CA, USA. However, garnets from this locality are referred to in the literature as titanian andradite or melanite (Moore and White 1971; Waychunas 1987; Lager et al. 1989; Armbruster et al. 1998). No chemical analysis is provided in

PDF 33-285, but a comment is made that a TiO_2 content of 13 wt% was determined by X-ray fluorescence, which is consistent with the reported unit-cell parameter (12.128 Å). Comparison with the published data (Armbruster et al. 1998; Wu and Mu 1986; Kühberger et al. 1989) shows that this amount of TiO_2 is insufficient to make Ti the predominant cation in the Y site. Consequently, we recommend that PDF 33-285 be replaced with new XRD data, e.g. those listed in Table 6 for schorlomite AF-05, which is well characterized both chemically and structurally (see Discussion).

Discussion

Cation distribution

Recalculation of the chemical analytical data on the stoichiometric basis, with all Ti cast as Ti^{4+} and H_2O (in sample AF-05) as hydroxyl groups, gives formulae with a significant deficit of Si atoms (ca. 25% of the total occupancy at Z). In the Afrikanda garnet, only 4% of that deficit can be accounted for with $(\text{OH})_4$ groups (Table 7). If the (remainder of) “missing” Si is compensated entirely with Fe^{3+} , the calculated electron density at Z exceeds the refined value by 5% in both AF-05 and MC-04, whereas the calculated electron density at the Y site is smaller than the refined density by 5%. Also, this model implies almost twice as much $^{44}\text{Fe}^{3+}$ as $^{66}\text{Fe}^{3+}$ and, hence, is at variance with the spectroscopic data (see above). These discrepancies clearly indicate that, in addition to Fe^{3+} , the Z site accommodates a lighter element or elements (e.g., Al and/or Ti). Attempts to compensate for the Si deficiency with Fe^{3+} and Ti^{4+} (i.e., following the model of Scordari et al. 1999) give unsatisfactory results because the calculated and refined electronic densities at the Y and Z sites differ by more than 3%. The best agreement between the calculated and refined epfu’s is achieved when some of the Si deficiency is compensated with Al (ca. 5–6% of the total occupancy at Z), Fe^{2+} is distributed between X and Y, and all Ti is assigned to Y. The X site is assumed to accommodate the largest cations in the order of decreasing radius (i.e., $\text{Na} > \text{Ca} > \text{Mn} > \text{Fe}^{2+}$). This cation-distribution model (Table 7) provides good agreement between the Y-O and Z-O distances calculated using the ionic radii of Shannon (1976)¹ and those obtained from the crystal-structure refinements (within 1% of the smallest value). The calculated X-O distances exceed the actual mean distances by about 2%. However, analysis of the literature shows that the X-O distance in Ti-rich granditic garnets is consistently smaller than that expected from the ionic radius of $^{88}\text{Ca}^{2+}$ (2.50 Å), and virtually insensitive to substitutions at the Y and Z sites. For example, garnets containing 6.9–

¹For $(\text{OH})_4$ tetrahedra in sample AF-05, a Z-O distance of 1.94 Å was used; it was calculated from the published data for “hydrogarnets” (Basso et al. 1983; Lager et al. 1987, 1989)

Table 5 Mössbauer spectroscopic data for schorlomite from Afrikanda and Magnet Cove: Comparison of hyperfine parameters for two different four-doublet fitting models to 80 K spectra

Doublets	Parameters	Sample AF-05		Sample MC-04	
		Model 1	Model 2	Model 1	Model 2
$^{44}\text{Fe}^{3+}$	CS (mm/s)	0.33(1)	0.34(1)	0.33(1)	0.33(1)
	QS (mm/s)	1.17(2)	1.15(2)	1.16(2)	1.15(2)
	σ (mm/s)	0.17(1)	0.17(1)	0.13(1)	0.13(1)
	area (%)	35(3)	38(3)	39(3)	41(3)
$^{60}\text{Fe}^{3+}$	CS (mm/s)	0.51(1)	0.50(1)	0.49(1)	0.48(1)
	QS (mm/s)	0.65(2)	0.66(2)	0.62(2)	0.66(2)
	σ (mm/s)	0.09(1)	0.08(1)	0.10(1)	0.10(1)
	area (%)	44(3)	41(3)	43(3)	41(3)
$^{56}\text{Fe}^{2+}$	CS (mm/s)	1.09(3)		1.09(3)	
	QS (mm/s)	2.05(5)		2.09(5)	
	Γ (mm/s)	0.63(2)		0.40(2)	
	area (%)	18(3)		15(3)	
$^{66}\text{Fe}^{2+}$	CS (mm/s)		1.19 ^a		1.19(3)
	QS (mm/s)		1.89(5)		1.91(5)
	Γ (mm/s)		0.58(2)		0.39(2)
	Area (%)		18(3)		15(3)
$^{80}\text{Fe}^{2+}$	CS (mm/s)	1.40(3)	1.40(3)	1.41(3)	1.41(3)
	QS (mm/s)	3.47(5)	3.49(5)	3.49(5)	3.51(5)
	Γ (mm/s)	0.25(2)	0.29(2)	0.31(2)	0.30(2)
	area (%)	3(1)	3(1)	3(1)	3(1)
	Reduced χ^2	1.4	1.6	1.6	1.7

Hyperfine parameters: CS center shift relative to α -Fe, QS quadrupole splitting, σ Gaussian width of QS distribution, Γ Lorentzian line width

^aThis value was held fixed during the fitting process

16.4 wt% TiO₂ all have an X-O distance of 2.44 Å (Wu and Mu 1986; Peterson et al. 1995; Armbruster et al. 1998; this work).

It is also noteworthy here that the refined epfu values at the X site exceed the calculated by 1–2% (Table 7); a similar “excess” of electron density has been documented for high-Ti andradite (12.4–12.9 wt% TiO₂) by Armbruster et al. (1998, their Table 5). Although this discrepancy is probably well within the accumulated analytical error, the fact that it has been observed in samples of different provenance suggests that it may be real and not fictitious. One possible explanation is that a small proportion of Zr is accommodated in the X site (ca. 1% of the total occupancy at X), because this element has a known affinity for high coordination (e.g., seven in baddeleyite and eight in zircon). Garnets with both $^{60}\text{Zr}^{4+}$ and $^{80}\text{Zr}^{4+}$ replacing Ca in the X site have been synthesized (Mill’ et al. 1966). In our case, a more accurate site-assignment for Zr is difficult due to its generally small concentration, and uncertainties in the distribution of other cations. Unfortunately, the high-Ti material of Armbruster et al. (1998) has not been analyzed for Zr.

Three of the doublets in the Mössbauer spectra collected at 80 K can be unambiguously assigned based on comparison of hyperfine parameter data at 80 and 293 K to the following: (1) Fe³⁺ in the Z site, (2) Fe³⁺ in the Y site, and (3) Fe²⁺ in the X site. The relative proportions of these spectroscopically distinct Fe species are in good agreement with those derived from the

structural analysis (Table 7). The fourth doublet, which is relatively well-resolved at 80 K, has center-shift values predominantly corresponding to tetrahedrally-coordinated Fe²⁺ (model 1) or octahedrally-coordinated Fe²⁺ (model 2). As can be seen from Table 5, the relative intensities of all four doublets are essentially identical for both models. The two narrow doublets in the room-temperature spectra can be assigned to Fe³⁺ in the Z and Y sites, respectively. The broad doublet has a center-shift of ca. 0.6 mm/s, which is intermediate between values for Fe²⁺ and Fe³⁺. Based on the published literature, this doublet likely represents an intermediate valence due to thermally activated electron delocalization. The intensity ratio $^{44}\text{Fe}^{3+}/^{60}\text{Fe}^{3+}$ is much smaller at room temperature than at 80 K (which is most easily seen by looking at the well-resolved low-velocity components), which implies that electron transfer involves Fe³⁺ in the Z site. From the structural constraints (Fig. 1), there are two possible routes for electron transfer involving tetrahedrally coordinated Fe³⁺: (1) $^{80}\text{Fe}^{2+} \leftrightarrow ^{44}\text{Fe}^{3+}$, and (2) $^{66}\text{Fe}^{2+} \leftrightarrow ^{44}\text{Fe}^{3+}$. The intensity data support the latter mechanism. Route (1) is inconsistent with the weak intensity of the $^{80}\text{Fe}^{2+}$ doublet at 80 K, whereas the relative area of the intermediate-valence doublet at room temperature is roughly equivalent to the total relative area reduction of the $^{44}\text{Fe}^{3+}$ and $^{66}\text{Fe}^{2+}$ doublets in going from 80 K to room temperature. We therefore favor assignment of the fourth doublet in the 80 K spectra to predominantly octahedrally coordinated Fe²⁺, which corresponds to our fitting model 2 (Table 5). The Fe²⁺/Fe_Σ values calculated from the EMPA analyses on the basis of stoichiometry, as well as the relative proportion between Fe²⁺ and Fe³⁺ assigned to the different sites using the structural and compositional data (see above), are within the estimated SD from the values derived from the Mössbauer spectra (Table 7). The calculated Fe²⁺/Fe_Σ ratios are, in fact, slightly lower than the measured Fe²⁺/Fe_Σ ratios for both AF-05 and MC-04, further indicating that our samples lack detectable Ti³⁺ (cf. Schwartz et al. 1980).

Table 6 XRD powder data for schorlomite from Afrikanda

d (Å)	I	hkl	d (Å)	I	hkl	d (Å)	I	hkl
4.30	2	220	1.685	22	640	1.227	1	941
3.247	1	321	1.653	1	633			853
3.038	74	400	1.624	52	642	1.128	6	10.4.0
2.717	100	420	1.519	5	800			864
2.590	7	332	1.500	1	741	1.109	13	10.4.2
2.480	38	422	1.432	1	822	1.074	6	880
2.383	10	431	1.358	33	840	1.012	6	12.0.0
2.218	12	521	1.326	13	842			884
1.971	8	611	1.310	1	921	0.999	9	12.2.0
		532	1.295	12	664	0.986	8	12.2.2
1.921	11	620	1.281	1	851			10.6.4
1.754	6	444			754			

$a = 12.1503(4)$ Å; $V = 1793.8(2)$ Å³. Five strongest lines are given in bold

Table 7 Crystal-chemical analysis of schorlomite: a summary

	Afrikanda sample AF-05			Magnet Cove sample MC-04		
	wt%	X site:	apfu	wt%	X site:	apfu
Na ₂ O	0.14	Na	0.023	0.12	Na	0.020
CaO	31.86	Ca	2.899	31.53	Ca	2.915
MnO	0.28	Mn	0.020	0.47	Mn	0.034
FeO ^a	3.60	Fe ²⁺	0.058	3.19	Fe ²⁺	0.031
MgO	1.23	Y site:		1.23	Y site:	
Al ₂ O ₃	2.20	Fe ²⁺	0.197	1.55	Fe ²⁺	0.200
Fe ₂ O ₃ ^a	16.48	Mg	0.156	17.10	Mg	0.158
SiO ₂	27.11	Al	0.049	26.22	Al	–
TiO ₂	15.02	Fe ³⁺	0.556	16.24	Fe ³⁺	0.530
ZrO ₂	1.93	Ti	0.959	1.34	Ti	1.054
Nb ₂ O ₅	0.07	Zr	0.080	0.05	Zr	0.056
H ₂ O ^b	0.21	Nb	0.003	n.d	Nb	0.002
Total	100.13	Z site:		99.04	Z site:	
		Si	2.302		Si	2.263
		Al	0.171		Al	0.157
		Fe ³⁺	0.497		Fe ³⁺	0.580
		H	0.119		H	–

Comparison of measured and calculated electron densities (epfu), cation- oxygen distances (Å), and Fe distribution among different sites (% of Fe_Σ):

	measured	calculated	X site	measured	calculated
X site			X site		
epfu	61.3(4)	60.2	epfu	60.8(4)	60.2
X-O	2.442(1)	2.496	X-O	2.442(1)	2.497
Y site			Y site		
epfu	46.7(3)	46.5	epfu	46.6(3)	46.4
Y-O	2.006(1)	2.025	Y-O	2.005(1)	2.025
Z site			Z site		
epfu	47.5(4)	47.5	epfu	48.5(4)	48.8
Y-O	1.689(1)	1.689	Y-O	1.693(1)	1.691
Fe ²⁺ /Fe _Σ	21(3)	19	Fe ²⁺ /Fe _Σ	18(3)	17
^[8] Fe ²⁺ /Fe _Σ	3(1)	4	^[8] Fe ²⁺ /Fe _Σ	3(1)	2
^[6] Fe ²⁺ /Fe _Σ	18(3)	15	^[6] Fe ²⁺ /Fe _Σ	15(3)	15
^[6] Fe ³⁺ /Fe _Σ	41(3)	43	^[6] Fe ³⁺ /Fe _Σ	41(3)	40
^[4] Fe ³⁺ /Fe _Σ	38(3)	38	^[4] Fe ³⁺ /Fe _Σ	41(3)	43

Mol% components

Schorlomite	29.2	Schorlomite	33.8
Andradite	26.7	Andradite	24.4
Morimotoite	19.7	Morimotoite	20.0
Ca ₃ (MgTi)Si ₃ O ₁₂	15.6	Ca ₃ (MgTi)Si ₃ O ₁₂	15.8
Kimzeyite	4.0	Kimzeyite	2.8
Other ^c	4.8	Other ^c	3.2

^aFeO and Fe₂O₃ values calculated from EMPA data assuming stoichiometry

^bwt% H₂O calculated as an average of three H analyses by combustion

^cIncluding (Na₂Ca)Ti₂Si₃O₁₂, Fe²⁺₃Fe³⁺₂Si₃O₁₂, calderite Mn²⁺₃Fe³⁺₂Si₃O₁₂, almandine Fe²⁺₃Al₂Si₃O₁₂, and katoite Ca₃Al₂(OH)₁₂ (< 1.5 mol% each)

The presence of thermally activated electron delocalization between ^[6]Fe²⁺ and ^[4]Fe³⁺ is unusual. Amthauer and Rossman (1984) conclude that, for such thermally activated electron transfer to take place, it must occur over essentially infinite structural units, where the cooperative exchange between a large number of Fe²⁺ and Fe³⁺ cations enables the activation energy to be decreased to the point where the transfer can occur at room temperature. Such structural units exist in the garnet structure, where corner-shared YO₆ octahedra and ZO₄ tetrahedra alternate. The ^[6]Fe²⁺–^[4]Fe³⁺ interatomic distance is ~3.40 Å, which is within the range over which electron transfer has been observed to occur (Burns 1993). Extended ^[6]Fe²⁺–^[4]Fe³⁺ units would

imply a degree of short-range order and, hence, local reduction of symmetry.

On the possibility of ^[4]Fe²⁺

It is noteworthy that there are some indications that the intermediate-valence doublet may represent Fe²⁺ in more than one coordination setting. The doublet center shift is slightly lower than typical values for ^[6]Fe²⁺ (ca. 1.25 mm/s at 80 K relative to α-Fe), and the linewidth is broader than that of the ^[8]Fe²⁺ doublet. This suggests that minor ^[4]Fe²⁺ is likely to be present in both garnets, although its amount cannot be quantified due to the lack

of spectral resolution. For example, the results for sample MC-04 (i.e., match between the calculated and measured epfu's) could be improved slightly by replacing ca. 0.025 apfu $^{44}\text{Fe}^{3+}$ with $^{44}\text{Fe}^{2+}$. However, this amount corresponds to less than 2% of Fe_Σ , which is well within the e.s.d. for $^{60}\text{Fe}^{2+}$ or $^{44}\text{Fe}^{3+}$ refined from the Mössbauer data. Hence, any "improvement" of the results presented in Table 7 through partial allocation of Fe^{2+} to the Z site would be speculative.

On the significance of $(\text{OH})^-$ groups

Very few Ti-rich garnets described in the literature have been analyzed for H_2O either chemically or using IR spectroscopy (e.g., Locock et al. 1995). On the basis of crystal-chemical arguments, Armbruster et al. (1998, p. 919) proposed that "crystals with dominant schorlomite substitution ... show only a low degree of additional hydrogarnet substitution ($\text{O}_4\text{H}_4 \Rightarrow \text{SiO}_4$)." Although this statement is generally true, especially when such schorlomic compositions are compared with hydrothermal/metamorphic andradite containing moderate levels of Ti (e.g., Flohr and Ross 1989; Lager et al. 1989), there are many examples where schorlomite crystallized from H_2O -rich melts, and can thus be expected to contain a fair proportion of $(\text{OH})^-$. Examples are carbonatitic magmas (such as produced the Afrikanda rock), melilititic, nephelinitic, alnöitic and other alkali-ultramafic magmas. Simple calculations show that even small amounts of unaccounted-for H_2O significantly affect the $\text{Fe}^{2+}/\text{Fe}_\Sigma$ ratio calculated from the EMPA data on the basis of stoichiometry. On average, each undetected $0.4(\text{OH})^-$, equivalent to 0.1 apfu of substituted Si, will give a 6% decrease in $\text{Fe}^{2+}/\text{Fe}_\Sigma$ ratio relative to the actual value.

On the schorlomite formula and inter-species boundaries

At present, there is no definitive, universally adopted formula for schorlomite; its compositional boundaries relative to other species (especially andradite) are not constrained either (Table 1). The inter-species boundaries defined in terms of wt% TiO_2 (e.g., Zedlitz 1933) have the following shortcomings:

1. They do not account for minor proportions of grossular, kimzeyite and other end-members commonly present in Ti-rich garnets, in which case garnets with $\text{TiO}_2 < 15$ wt% may still show the prevalence of schorlomite over andradite.
2. They do not account for the Ti components other than schorlomite; however questionable the status of morimotoite, there is no doubt that the $\text{Fe}^{2+}\text{Ti}^{4+}\text{Fe}^{3+}_{-2}$ and $\text{MgTi}^{4+}\text{Fe}^{3+}_{-2}$ substitutions are ubiquitous in Ti-rich garnets (see above).
3. They are inapplicable to compositions with low or high analytical totals; given that Ti-rich garnets may contain H_2O , and garnet analyses are usually re-

ported with total Fe as either FeO or Fe_2O_3 , appreciable deviations of analytical totals from 100% are not uncommon in the literature.

Another commonly used discriminant is the prevalence of Ti over Fe^{3+} in the Y site (Deer et al. 1982). This criterion enables the distinction of schorlomite from andradite, but does not account for $\text{Fe}^{2+}\text{Ti}^{4+}\text{Fe}^{3+}_{-2}$ and other alternative substitutions involving $^{60}\text{Ti}^{4+}$; for example, the morimotoite of Henmi et al. (1995) also has $^{60}\text{Ti} > ^{60}\text{Fe}^{3+}$.

The end-member formula of Ito and Frondel (1967) is an accurate reflection of the schorlomite crystal chemistry in that it shows $\text{Ti}^{4+}\text{Fe}^{3+}\text{Fe}^{3+}_{-1}\text{Si}_{-1}$ to be the principal substitution in this mineral (e.g., Table 7). However, this formula is ambiguous: it may be interpreted as stipulating that a garnet has both $^{60}\text{Ti} > ^{60}\text{Fe}^{3+}$ and $^{44}\text{Fe}^{3+} > ^{44}\text{Si}$ to be termed schorlomite. None of the published schorlomite analyses meet the latter requirement, with the overwhelming majority of compositions having 2.05–2.35 apfu Si (Lupini et al. 1992; Locock et al. 1995, among others). The most Ti-rich composition reported to date (Grapes et al. 1979) has 1.8 apfu Si if recalculated on the stoichiometric basis, but this single analysis is most likely at error, as indicated by the anomalously low Ca and high Fe^{2+} contents (1.5 and 2.2 apfu, respectively). Given that this garnet replaces ilmenite (ibid.), it is likely that the reported EMPA data were "contaminated" by excitation of the ilmenite, which would readily explain the high Fe^{2+} and Ti, but low Ca and Si contents. It is noteworthy that Si deficiency increases proportionately with Zr content, reaching $\geq 50\%$ of the total Z-site occupancy in kimzeyite (Lupini et al. 1992, their Fig. 1).

Another weakness of the formula-based nomenclatural approach is that Fe^{3+} is not the only substituent in the Z site. Despite the ambiguities in interpretation of structural and spectroscopic data, there seems little doubt that both Al^{3+} and Fe^{2+} can also enter this site (see the discussion above). If schorlomite is defined as one of the three potential end-members, i.e. $\text{Ca}_3\text{Ti}^{4+}_2(\text{Fe}^{3+}_2\text{Si})\text{O}_{12}$, $\text{Ca}_3\text{Ti}^{4+}_2(\text{Al}_2\text{Si})\text{O}_{12}$ or $\text{Ca}_3\text{Ti}^{4+}_2(\text{Fe}^{2+}_2\text{Si}_2)\text{O}_{12}$, none of the schorlomite samples described in the literature, for which site occupancies are reasonably well constrained, will have enough of any one of these components to outbalance the proportion of andradite. For example, sample AF-05 would have to be termed andradite because it contains ca. 25 mol% $\text{Ca}_3\text{Ti}^{4+}_2(\text{Fe}^{3+}_2\text{Si})\text{O}_{12}$, 9 mol% $\text{Ca}_3\text{Ti}^{4+}_2(\text{Al}_2\text{Si})\text{O}_{12}$ and 28 mol% $\text{Ca}_3\text{Fe}^{3+}_2\text{Si}_3\text{O}_{12}$, and MC-04 would only marginally qualify as schorlomite.

Taking into consideration the above arguments, we propose that schorlomite be defined as a calcic garnet, in which (1) Ti^{4+} is the predominant cation in the Y site, and (2) the incorporation of Ti^{4+} in this site is balanced predominantly by substitution of Si by lower-charged cations (especially Fe^{3+} and Al) in the Z site. Condition (1) distinguishes schorlomite from andradite, kimzeyite and grossular, whereas condition (2) allows us

to discriminate between schorlomite and other garnets in which the accommodation of Ti^{4+} in the structure is accompanied by substitutions in the X or Y site, i.e. $\text{NaTi}^{4+}\text{Ca}_{-1}\text{Fe}^{3+}_{-1}$, $\text{Fe}^{2+}\text{Ti}^{4+}\text{Fe}^{3+}_{-2}$, and $\text{MgTi}^{4+}\text{Fe}^{3+}_{-2}$. Among the three garnets defined by these substitutions, only $\text{Ca}_3(\text{Fe}^{2+}\text{Ti}^{4+})\text{Si}_3\text{O}_{12}$ has been described as a mineral species (morimotoite). Garnets, in which $\text{Ca}_3(\text{MgTi}^{4+})\text{Si}_3\text{O}_{12}$ is the predominant component, can potentially exist in nature, especially in such Mg–Ti-rich settings as rodingites and other strongly metasomatized meta-(ultra)mafic rocks. $(\text{Na}_2\text{Ca})\text{Ti}^{4+}_2\text{Si}_3\text{O}_{12}$ is not likely to be the principal component in any naturally occurring garnets because of significant mismatch between the large NaO_8 and small TiO_6 polyhedra.

Thus, the generalized formula of schorlomite may be written as $\text{Ca}_3\text{Ti}^{4+}_2[\text{Si}_{3-x}(\text{Fe}^{3+}, \text{Al}, \text{Fe}^{2+})_x\text{O}_{12}]$, where the order of elements in parentheses reflects their relative abundance (i.e. $\text{Ti}^{4+}\text{Fe}^{3+}\text{Fe}^{3+}_{-1}\text{Si}_{-1}$ is the principal substitution mechanism). The published analyses of schorlomite all have $x = 0.6\text{--}1.0$, although the available experimental data (e.g., Povarennykh and Shabalin 1983) indicate that compositions with $x > 1.0$ may also exist. We purposefully omitted $^{6}\text{Ti}^{3+}$ and $^{4}\text{Ti}^{4+}$ from the proposed formula because, in our opinion, neither has been conclusively demonstrated to exist in natural schorlomite (Waychunas 1987; Locock et al. 1995; this work).

The mole percentage of schorlomite component can be determined as the proportion of $^{6}\text{Ti}^{4+}$ (apfu) balanced by substitutions in the Z site, relative to the total amount of cations in the Y site: $(^{6}\text{Ti}^{4+}_{-1}[^{6}\text{Fe}^{2+}_{-1}[^{6}\text{Mg}^{2+}_{-1}[^{8}\text{Na}^{+}]]])/2$ (Table 7). Our calculations show that schorlomite, andradite, morimotoite and $\text{Ca}_3(\text{MgTi}^{4+})\text{Si}_3\text{O}_{12}$ (Mg-analogue of morimotoite) are the major components in both AF-05 and MC-04, kimzeyite is present in appreciable amounts, and other garnet-type components total less than 5 mol%. In accord with the crystal-chemical considerations (Armbruster et al. 1998), we used for kimzeyite the end-member formula $\text{Ca}_3\text{Zr}_2(\text{Al}_2\text{Si})\text{O}_{12}$. Natural kimzeyite invariably contains a significant proportion of $\text{Ca}_3\text{Zr}_2(\text{Fe}^{3+}_2\text{Si})\text{O}_{12}$ (e.g., Schingaro et al. 2001), indicating that our discussion of schorlomite formula may also be relevant to this mineral. Clearly, the choice of kimzeyite formula will not affect the mole proportion of schorlomite calculated using the above-described approach.

That schorlomite cannot be assigned a definite end-member formula is not irrational, and nor is it unique to this mineral species. There is actually a great number of minerals (most of the rare-earth phases, pyrochlores, Ca-deficient clinopyroxenes, etc.), whose crystal chemistry is so complex that it can only be defined in terms of two or more end-members, whereas near-end-member compositions are unlikely to be ever found in nature.

Tentative identification of Ti-rich garnets from EMPA

Ultimately, a multi-analytical study involving spectroscopic and single-crystal diffraction methods, would be

required to establish with certainty whether a Ti-rich garnet is schorlomite. However, if site-occupancy data are unavailable, the approximate schorlomite content can be estimated from EMPA-based stoichiometric formula (i.e., 12 oxygen atoms and eight cations), in which cations have been assigned to the individual sites in the following order:

1. ^{8}X site: $\text{Na} + \text{Ca} + \text{Mn} + \text{Fe}^{2+}$ required to bring the cation total to 3
2. ^{4}Z site: $\text{Si} + \text{Al} + \text{Fe}^{3+}$ required to bring the cation total to 3
3. ^{6}Y site: $\text{Zr} + \text{Ti} + \text{Nb} + \text{Mg} + \text{Mn}$ [leftover from (1)] + Fe^{2+} [leftover from (1)] + Fe^{3+} [leftover from (2)]. Other elements that could potentially be present in Ti-rich garnets in minor quantities, should be assigned as follows: lanthanides, Y and Th to the X site; V, Cr, Sn and Hf to the Y site; P and S to the Z site.

Although this approach does not account for $^{4}\text{Fe}^{2+}$, our data show that its proportion is small and comparable to the accuracy of $\text{Fe}^{2+}/\text{Fe}^{3+}$ measurements by spectroscopic techniques (i.e., $\sim 3\%$ Fe^{2+}). The above method will give higher-than-actual morimotoite (and lower schorlomite) contents for samples containing significant $^{4}\text{Fe}^{2+}$, which, in our opinion, has not been conclusively demonstrated for any of the Ti-rich garnets studied to date. Unaccounted-for water is of greater concern as it will produce spurious $\text{Fe}^{2+}/\text{Fe}^{3+}$ results (see above) and, in addition, higher-than-actual apfu values for all other cations. In some cases, the presence of undetected H_2O can be readily recognized from unrealistic Ca contents exceeding 3 apfu, as neither Y nor Z site can accommodate any Ca (cf. Müntener and Hermann 1994). Distinctly birefringent garnets should also be suspect of containing $(\text{OH})^-$ groups (e.g., Flohr and Ross 1989; Ulrych et al. 1994). With these reservations in mind, the proposed calculation method can be reasonably used for *provisional* identification. For example, the schorlomite, andradite and morimotoite contents of sample AF-05 calculated from the average analysis (Table 1) on a water-free basis deviate from the values in Table 7 by +1.1, +2.1 and -1.6 mol%, respectively. In many cases, such minor deviations are probably comparable to variations due to analytical errors and/or compositional heterogeneity of crystals. However, any petrogenetic study building on the composition of titanian garnets [e.g., studies of magma-fractionation trends or $f(\text{O}_2)$ evolution in the melt] must involve an independent determination of $\text{Fe}^{2+}/\text{Fe}^{3+}$ and H_2O by spectroscopic or other analytical methods.

Conclusions

Examination of two schorlomite samples from different rocks (one from the type locality at Magnet Cove) using a combination of analytical methods, and comparison of

these data with those available in the literature show that:

1. Incorporation of Ti in the garnet structure involves several substitution mechanisms, i.e., $\text{NaTi}^{4+}\text{Ca}_{-1}\text{Fe}^{3+}_{-1}\text{Fe}^{2+}\text{Ti}^{4+}\text{Fe}^{3+}_{-2}\text{Mg}^{2+}\text{Ti}^{4+}\text{Fe}^{3+}_{-2}\text{Ti}^{4+}\text{Fe}^{3+}\text{Fe}^{3+}_{-1}\text{Si}_{-1}$, $\text{Ti}^{4+}\text{Al}^{3+}\text{Fe}^{3+}_{-1}\text{Si}_{-1}$, and $\text{Ti}^{4+}_2\text{Fe}^{2+}\text{Fe}^{3+}_{-2}\text{Si}_{-1}$.
2. $\text{Ti}^{4+}\text{Fe}^{3+}\text{Fe}^{3+}_{-1}\text{Si}_{-1}$ is the principal substitution in schorlomite, followed by $\text{Ti}^{4+}\text{Al}^{3+}\text{Fe}^{3+}_{-1}\text{Si}_{-1}$; $^{44}\text{Fe}^{2+}$ is present in minor quantities that cannot be quantified by the conventional Mössbauer techniques. Although $^{44}\text{Ti}^{4+}$ cannot be ruled out conclusively, the spectroscopic data, observed electron densities and cation-anion distances at the Z site are best explained by accommodation of Fe^{3+} and Al in this site, rather than any combination involving Ti^{4+} . This observation is in agreement with the near-edge X-ray absorption spectroscopic data of Waychunas (1987) and Locock et al. (1995).
3. Our interpretation of the Mössbauer spectra as indicating thermally activated electron delocalization between $^{60}\text{Fe}^{2+}$ and $^{44}\text{Fe}^{3+}$ agrees with the spectroscopic analysis of Ti-rich garnets (9.7–15.3 wt% TiO_2) from China (Wu and Mu 1986), but is at variance with the interpretation offered for the Ice River schorlomite by Locock et al. (1995). Assignment of the doublet with a center shift of 1.1–1.2 mm/s to $^{44}\text{Fe}^{2+}$, as proposed in the latter study, would be inconsistent with the observed electron densities and cation-anion distances at the Y and Z sites.
4. The crystallographic data, as well as good correspondence between the $\text{Fe}^{2+}/\text{Fe}_\Sigma$ values measured from the Mössbauer spectra and those calculated from EMPA assuming stoichiometry, indicate that our schorlomite samples lack detectable Ti^{3+} . This conclusion is in accord with the near-edge X-ray absorption spectroscopic data of Waychunas (1987) and Locock et al. (1995).
5. Na and Zr are common substituents in Ti-rich garnets and should be included in the chemical analysis.
6. The formula of schorlomite may be generalized as $\text{Ca}_3\text{Ti}^{4+}_2[\text{Si}_{3-x}(\text{Fe}^{3+}, \text{Al}, \text{Fe}^{2+})_x\text{O}_{12}]$; for classification purposes, the mole percentage of schorlomite is determined as the amount of $^{60}\text{Ti}^{4+}$, balanced by substitutions in the Z site, relative to the total occupancy in the Y site: $(^{60}\text{Ti}^{4+}_{-60}\text{Fe}^{2+}_{-60}\text{Mg}^{2+}_{-80}\text{Na}^+) / 2$.
7. Provisional identification of a garnet as schorlomite or titanian andradite can be done on the basis of electron-microprobe analyses recalculated to a stoichiometric formula, i.e., $\text{X}_3\text{Y}_2\text{Z}_3\text{O}_{12}$. However, the atomic amounts of Fe^{2+} , Fe^{3+} , Ti^{4+} and Si^{4+} so obtained cannot be used as a basis for petrogenetic analysis. It is essential to constrain at least some of these compositional variables using spectroscopic and crystallographic methods.

Acknowledgements This work was supported in part by the Natural Sciences and Engineering Research Council of Canada (ARC). Mössbauer experiments were performed using the equipment purchased with funds awarded to F. Seifert by Fonds der Chemischen Industrie (Germany) under the “Materials Research” program. Mike Howard is cordially thanked for providing us with a collection of Magnet Cove garnets (including sample MC-04) and details on their geological provenance. We are very grateful to Mark Cooper for his help with the collection, processing and interpretation of the single-crystal data, and for his comments on the earlier draft of this paper. This study would not have been possible without the kind permission of Frank C. Hawthorne to use the single-crystal X-ray facility at the University of Manitoba, equipped through Major Equipment and Equipment grants from the Natural Sciences and Engineering Research Council of Canada to FCH. We are also grateful to Ron Chapman, Keith Pringnitz and Allan MacKenzie for their help with the analytical work, and to Anne Hammond for the masterfully executed thin sections. This manuscript has benefited from many constructive comments made by two anonymous reviewers, Giovanni Ferraris and editor James Tyburczy.

References

- Amthauer G, Rossman GR (1984) Mixed valence of iron in minerals with cation clusters. *Phys Chem Minerals* 11:37–51
- Amthauer G, Annersten H, Hafner SS (1977) The Mössbauer spectrum of ^{57}Fe in titanium-bearing andradites. *Phys Chem Minerals* 1:399–413
- Anthony JW, Bideaux RA, Bladh KW, Nichols MC (1995) Handbook of mineralogy, vol II: Silica, silicates. Part 2. Mineral Data Publ, Tucson
- Armbruster T, Geiger CA (1993) Andradite crystal chemistry, dynamic X-site disorder and structural strain in silicate garnets. *Eur J Mineral* 5:59–71
- Armbruster T, Birrer J, Libowitzky E, Beran A (1998) Crystal chemistry of Ti-bearing andradites. *Eur J Mineral* 10:907–921
- Basso R, Della Giusta A, Zefiro L (1983) Crystal structure refinement of plazolite: a highly hydrated natural hydrogrossular. *Neues Jahrb Mineral Monatsh* 1983:251–258
- Brod JA, Junqueira-Brod TC, Gaspar JC, Gibson SA, Thompson RN (2003) Ti-rich and Ti-poor garnet from the Tapira carbonatite complex, SE Brazil: Fingerprinting fractional crystallization and liquid immiscibility. In: 8th Inter Kimb Conf Ext Abstr CD, file FLA_0339.pdf
- Burns RG (1993) Mineralogical applications of crystal field theory. Cambridge University Press, Cambridge
- Chakhmouradian AR, Zaitsev AN (2002) Calcite-amphibole-clinopyroxene rock from the Afrikanda complex, Kola Peninsula, Russia: mineralogy and a possible link to carbonatites. III. Silicate minerals. *Can Mineral* 40:1347–1374
- Chakhmouradian AR, Zaitsev AN (2004) Afrikanda: An association of ultramafic, alkaline and alkali-silica-rich carbonatitic rocks from mantle-derived melts. In: Wall F, Zaitsev AN (eds) Phoscorites and carbonatites from mantle to mine: the key example of the Kola Alkaline Province, Mineralogical Society (UK) Series, 10, pp 247–291
- Dawson JB, Smith JV, Steele IM (1995) Petrology and mineral chemistry of plutonic igneous xenoliths from the carbonatite volcano, Oldoinyo Lengai, Tanzania. *J Petrol* 36:797–826
- Deer WA, Howie RA, Zussman J (1982) Rock-forming minerals, vol 1A: Orthosilicates. Longman, New York
- Fehr KT, Amthauer G (1996) In: Henmi et al. (1995) (ed) Comment on ‘Morimotoite, $\text{Ca}_3\text{TiFe}^{2+}\text{Si}_3\text{O}_{12}$, a new titanian garnet from Fuka, Okayama Prefecture, Japan. *Mineral Mag* 60:842–845

- Flohr MJK, Ross M (1989) Alkaline igneous rocks of Magnet Cove, Arkansas: Metasomatized ijolite xenoliths from Diamond Jo quarry. *Am Mineral* 74:113–131
- Gaines RV, Skinner HCW, Foord EE, Mason B, Rosenzweig A (1997) Dana's new mineralogy. Wiley, New York
- Grapes RH, Yagi K, Okumura K (1979) Aenigmatite, sodic pyroxene, arfvedsonite and associated minerals in syenites from Morotu, Sakhalin. *Contrib Mineral Petrol* 69:97–103
- Gwalani LG, Rock NMS, Ramasamy R, Griffin BJ, Mulai BP (2000) Complexly zoned Ti-rich melanite-schorlomite garnets from Ambadungar carbonatite-alkalic complex, Deccan Igneous Province, Gujarat State, Western India. *J Asian Earth Sci* 18:163–176
- Hammond AL, Mitchell RH (2002) Accessory mineralogy of orangeite from Swaruggens, South Africa. *Mineral Petrol* 76:1–19
- Henmi C, Kusachi I, Henmi K (1995) Morimotoite, $\text{Ca}_3\text{TiFe}^{2+}\text{-Si}_3\text{O}_{12}$, a new titanian garnet from Fuka, Okayama Prefecture, Japan. *Mineral Mag* 59:115–120
- Holland TJB, Redfern SAT (1997) Unit cell refinement from powder diffraction data: the use of regression diagnostics. *Mineral Mag* 61:65–77
- Howie RA, Woolley AR (1968) The role of titanium and the effect of TiO_2 on the cell size, refractive index, and specific gravity in the andradite-melanite-schorlomite series. *Mineral Mag* 36:775–790
- Huggins FE, Virgo D, Huckenholz HG (1977) Titanium-containing silicate garnets. I. The distribution of Al, Fe^{3+} , and Ti^{4+} between octahedral and tetrahedral sites. *Am Mineral* 62:475–490
- Ibers JA, Hamilton WC, eds (1992) International tables X-ray crystallography, vol IV. Kynoch, Birmingham
- Ito J, Frondel C (1967) Synthetic zirconium and titanium garnets. *Am Mineral* 52:773–781
- Kühberger A, Fehr T, Huckenholz HG, Amthauer G (1989) Crystal chemistry of a natural schorlomite and Ti-andradites synthesized at different oxygen fugacities. *Phys Chem Minerals* 16:734–740
- Kukharensko AA, Bagdasarov EA (1962) Paragenesis and crystal-chemical characteristics of titanian garnets from alkali-ultramafic rocks of the Kola Peninsula (in Russian) *Uchenye Zapiski LGU. Ser Geolog* 13:115
- Lager GA, Armbruster T, Faber J (1987) Neutron and X-ray diffraction study of hydrogarnet $\text{Ca}_3\text{Al}_2(\text{O}_4\text{H}_4)_3$. *Am Mineral* 72:756–765
- Lager GA, Armbruster T, Rotella FJ, Rossman GR (1989) OH substitution in garnets: X-ray and neutron diffraction, infrared, and geometric-modeling studies. *Am Mineral* 74:840–851
- Lehijarvi M (1960) The alkaline district of Iivaara, Kuusamo, Finland. *Bull Comm Geol Finl* 185:62
- Locock A, Luth RW, Cavell RG, Smith DGW, Duke MJM (1995) Spectroscopy of the cation distribution in the schorlomite species of garnet. *Am Mineral* 80:27–38
- Lupini L, Williams CT, Woolley AR (1992) Zr-rich garnet and Zr- and Th-rich perovskite from the Polino carbonatite, Italy. *Lithos* 56:581–586
- Malitesta C, Losito I, Scordari F, Schingaro E (1995) XPS investigation of titanium in melanites from Monte Vulture (Italy). *Eur J Mineral* 7:847–858
- Mill' BV, Zadneprovskii GM, Bakakin VV (1966) New compounds with structures of the garnet type. *Izv Akad Nauk SSSR, Neorg Mater* 2:1861–1864
- Moore RK, White WB (1971) Intervalence electron charge transfer effects in the spectra of the melanite garnets. *Am Mineral* 56:826–840
- Müntener O, Hermann J (1994) Titanian andradite in a metapyroxenite layer from the Malenco ultramafics (Italy): implications for Ti-mobility and low oxygen fugacity. *Contrib Mineral Petrol* 116:156–168
- Peterson RC, Locock AJ, Luth RW (1995) Positional disorder of oxygen in garnet: the crystal-structure refinement of schorlomite. *Can Mineral* 33:627–631
- Povarennykh AS, Shabalin BG (1983) Structural role of titanium and iron in synthetic zirconium- and titanium-bearing garnets (in Russian). *Geol Zhurnal* 43:45–50
- Rass IT (1997) Morimotoite, a new titanian garnet?—discussion. *Mineral Mag* 61:728–730
- Rass IT, Dubrovinskii LS (1997) The thermodynamic parameters and stability region of schorlomite. *Trans (Doklady) Russ Acad Sci Earth Sci Sect* 355:730–732
- Rickwood PC (1968) On recasting analyses of garnet into end-member molecules. *Contrib Mineral Petrol* 18:175–198
- Roberts WL, Rapp GR, Weber J (1974) Encyclopedia of Minerals. Van Nostrand Reinhold, New York
- Russell JK, Dipple GM, Lang JR, Lueck B (1999) Major-element discrimination of titanian andradite from magmatic and hydrothermal environments: an example from the Canadian Cordillera. *Eur J Mineral* 11:919–935
- Schingaro E, Scordari F, Capitanio F, Parodi G, Smith DC, Mottana A (2001) Crystal chemistry of kimzeyite from Anguillara, Mts. Sabatini, Italy. *Eur J Mineral* 13:749–759
- Schwartz KB, Nolet DA, Burns RG (1980) Mössbauer spectroscopy and crystal chemistry of natural Fe–Ti garnets. *Am Mineral* 65:142–153
- Scordari F, Schingaro E, Pedrazzi G (1999) Crystal chemistry of melanites from Mt. Vulture (Southern Italy). *Eur J Mineral* 11:855–869
- Shannon RD (1976) Revised effective ionic radii and systematic studies of interatomic distances in halides and chalcogenides. *Acta Crystallogr* A32:751–767
- Shepard CU (1846) On three new mineral species from Arkansas, and the discovery of the diamond in North Carolina. *Am J Sci* 2:249–254
- Ulrych J, Povondra P, Pivec E, Rutšek J, Sitek J (1994) Compositional evolution of metasomatic garnet in melilitic rocks of the Osečná complex, Bohemia. *Can Mineral* 32:637–647
- Waychunas GA (1987) Synchrotron radiation XANES spectroscopy of Ti in minerals: effects of Ti bonding distances, Ti valence, and site geometry on absorption edge structure. *Am Mineral* 72:89–101
- Wu G, Mu B (1986) The crystal chemistry and Mössbauer study of schorlomite. *Phys Chem Minerals* 13:198–205
- Yakovenchuk VN, Ivanyuk GYu, Pakhomovskiy YaA, Men'shikov YuP (1999) Minerals of the Khibina Massif (in Russian). *Zemlya, Moscow*
- Yakovlevskaya TA (1972) The garnet group (in Russian). In: Chukhrov FV (ed) *Minerals*. vol III, Issue 1. Nauka, Moscow, pp 17–85
- Zedlitz O (1933) Über titanreichen Kalkeisengranat. *Zentralbl Mineral* 1933A:225–239